International Cartographic Association
Association Cartographique Internationale

Mapping the restoration process of coastal forests damaged by the 2011 tsunami using NDVI and LAI from time-series high-resolution satellite data

Hideki Hashiba [a,*], Masashi Sonobe [a]

[a] *Dept. of Civil Engrg, Coll. of Sci. and Tech., Nihon Univ., Japan - hashiba.hideki@nihon-u.ac.jp, sonobe.masashi@nihon-u.ac.jp*
* Corresponding author

Abstract: Approximately 14 years have passed since the large-scale Great East Japan Earthquake that occurred in the Tohoku region of Japan. For coastal disaster prevention, coastal forests, mainly consisting of black pine trees, had been developed over a wide area before the earthquake and were maintained by the Forestry Agency and local governments. The huge tsunami caused severe damage to these coastal forests, including fallen and lost trees. In order to progress in the restoration of coastal forests, it is necessary to effectively map the process over time. In this study, by using time-series high-resolution satellite remote sensing by Worldview-2,3 and GeoEye-1, the time-series changes in the afforestation area over a long period of approximately 12 years from before the disaster to immediately after the disaster and thereafter were mapped in detail by interpretation survey of high-resolution satellite images and analysis of the normalized difference vegetation index (NDVI). Furthermore, by using the conversion formula from NDVI to the leaf area index (LAI) reported in previous studies, an attempt was made to evaluate the restoration process of coastal forests from the disaster using LAI mapping. As a result, the process of restoration of coastal forests from the tsunami damage was effectively demonstrated through image interpretation and the characteristics of the spatial distribution of both index values.

Keywords: Coastal forest, disaster restoration, high resolution satellite image, NDVI, LAI

1. Introduction

About 14 years have passed since the Great East Japan Earthquake, which occurred mainly in the Tohoku region of Japan and was accompanied by a huge tsunami, and recovery and reconstruction are progressing in the affected areas. The Sendai Plain, located on the coast of Sendai City, Miyagi Prefecture, close to the epicenter, has a long coastline from north to south and suffered severe damage from the huge tsunami caused by the earthquake at that time. Coastal forests, mainly planted with black pine trees for coastal disaster prevention, were developed along the coastline of the Sendai Plain and maintained by the Forestry Agency and local governments. The huge tsunami caused by the Great East Japan Earthquake caused severe damage to this coastal forest over a wide area, including fallen trees and washout. In order to restore this coastal forest after the disaster, a long-term reforestation restoration project has been underway, centered on the Forestry Agency and Miyagi Prefecture. As the project progresses, it is necessary to effectively monitor the growth and changes in the condition of the reforestation. In addition, it is necessary to appropriately evaluate the progress of the reforestation project. Satellite remote sensing has an advantage in wide-area, periodic, and long-term time-series surveys. In particular, optical satellite observations with high spatial resolution allow for more detailed surveys of tree growth environments. In addition, many vegetation index values have been proposed based on the observation characteristics of different wavelength bands using multi-band multispectral image data, including the near-infrared light region, and many surveys of vegetation activity have been conducted. To date, Hashiba, H. et al. (2015), Sonobe, M. et al. (2018) have been promoting the use of NDVI (the Normalized Difference Vegetation Index proposed by Rouse, J. et al. (1974)) based on high-resolution satellite image data to evaluate afforestation in the disaster-stricken areas. In addition, the applicability of improved vegetation indices MSAVI-2 proposed by Qi,J. et al. (1994) and EVI-2 proposed by Jiang, Z. et al. (2008) has been examined, and the effectiveness of these vegetation index values for afforestation surveys in disaster-stricken areas has been reported by Hashiba, H. et al. (2024). On the other hand, the leaf area index (LAI) for evaluating the growth and lushness of foliage has been widely examined in relation to NDVI measured by field measurements and satellite images. The correlation between vegetation index values from satellite data analysis and measured LAI has been confirmed to some extent, and various LAI estimation formulas have been proposed. Regarding the relationship between NDVI from satellite image analysis and LAI from field measurements, Hoshi, N. et al. (2001) proposed a relational equation between NDVI and LAI obtained from observation images from the TM sensor of the medium-resolution satellite Landsat-5, and Kimm, H. et al. (2015) proposed a relational equation between NDVI and LAI obtained from observation images from the OLI sensor of Landsat-8. In addition, Kokubo, Y. et al. (2020) have proposed a relational equation between NDVI and LAI obtained from observation images from the high-resolution satellite Worldview-2. Thus, there have been many studies on forest foliage growth using measured LAI and estimation research using satellite data, but there have been no cases in which LAI estimates obtained from high-resolution satellite data have been used to evaluate the restoration process of coastal forests from tsunami damage.

In this study, time-series high-resolution satellite remote sensing by Worldview-2, 3 and GeoEye-1 was used to map in detail the time-series changes in the entire afforestation area from before the disaster to immediately after the disaster, and over a long period of approximately 12 years thereafter, using NDVI. Furthermore, by using a previously reported conversion formula from satellite image data to LAI, the damage to coastal forests and the restoration process were evaluated by mapping the time-series changes in LAI. As a result, the long-term restoration process of the afforestation area damaged by the tsunami was mapped in more detail in terms of both NDVI and LAI. The results also considered the characteristics of vegetation index values for long-term monitoring of the afforestation process in coastal forest areas damaged by the tsunami.

2. Research Methods

2.1 Research Area

The Great East Japan Earthquake occurred on March 11, 2011, and the magnitude of the earthquake was recorded as 9.0 on the Richter scale. In addition to the damage to buildings caused by the earthquake, the huge tsunami generated by the earthquake caused damage to coastal forests and widespread flooding in the coastal areas of the Tohoku region. The area covered by the analysis here was a 10km x 2.5km area along the coastline of the Sendai Plain in Miyagi Prefecture (Figure.1). In this area, many coastal forests that had been developed for disaster prevention purposes were damaged by the tsunami, falling and being washed away. In the area, coastal forests, mainly black pine plantations, have been maintained for many years. The development and maintenance of these plantations is divided into areas under the jurisdiction of national forests and private forests, and the plantations are managed in each area (Figure.2). The area to be surveyed and analyzed in this study was set as the afforestation area, which included both of these management areas.

2.2 Satellite image data

Here, satellite image data with a spatial resolution of 2.0m x 2.0m in the multispectral band observed by the high-resolution satellites Worldview-2, 3 and GeoEye-1 were used. In order to understand the long-term changes in the coastal forests since before the disaster, a total of seven scenes of data observed in spring at intervals of about 2 to 4 years before and after the disaster were used. A list of the data used is shown in Table 1. The observed multispectral images were 4 bands in the case of GeoEye-1 and 8 bands in the case of Worldview-2, 3. When analyzing the vegetation index values, image data in the visible red and near-infrared bands were used for analysis. Near-infrared images of band 4 were used in the case of GeoEye-1, and band 7 in the case of Worldview-2, 3. Detailed values for the observed wavelength bands of each data are shown in Table 2.

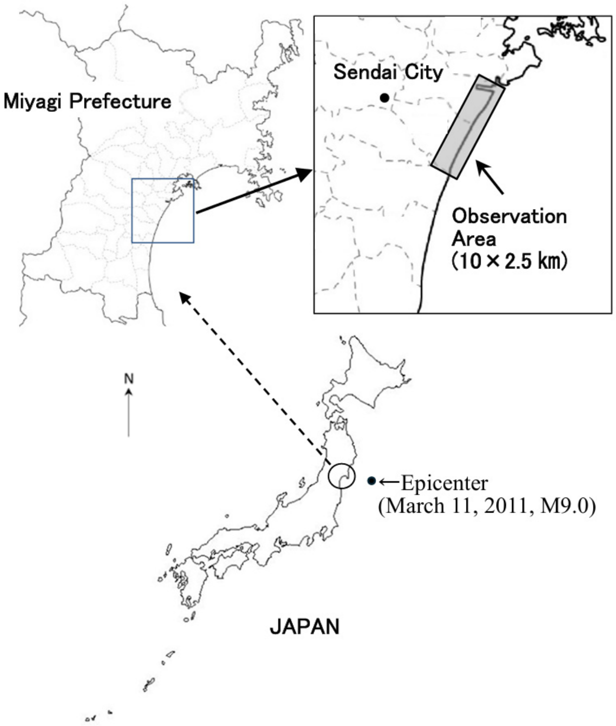

Figure 1. Research region and satellite image data range

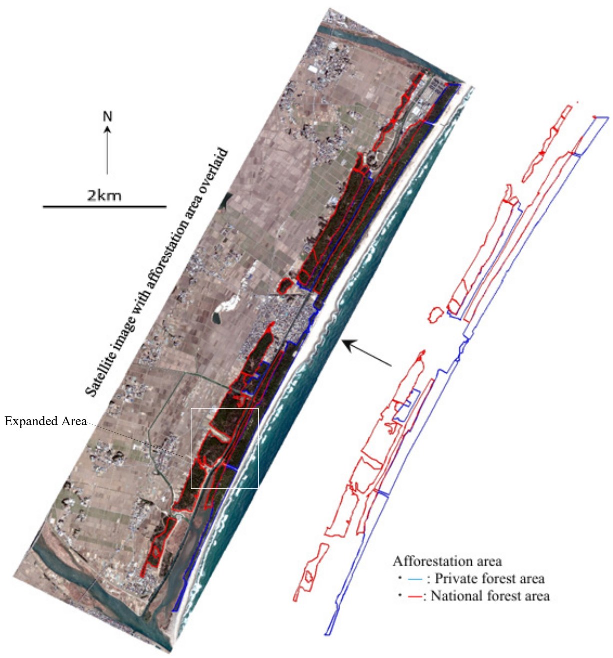

Figure 2. Research area and extent of afforestation

Acquisition date	Satellite	Band	Spatial Resolution	Remarks
2010/4/4	GeoEye-1	4 band Multi Spectral	2m×2m	Before disaster
2011/3/14	GeoEye-1	4 band Multi Spectral	2m×2m	Three days after the disaster
2013/4/14	GeoEye-1	8 band Multi Spectral	2m×2m	
2014/4/2	Worrdview-2	8 band Multi Spectral	2m×2m	3 years after the disaster
2016/4/13	Worrdview-3	8 band Multi Spectral	2m×2m	
2020/4/8	Worrdview-2	8 band Multi Spectral	2m×2m	
2023/3/31	Worrdview-2	8 band Multi Spectral	2m×2m	12 years after the disaster

Table 1. Specifications of satellite imagery data used

GeoEye-1 (GeoEye Imaging System（GIS）)

Band	Bandwidth	Wavelength
Band1	Visible Blue	450～510nm
Band2	Visible Green	520～580nm
Band3	Visible Red	655～690nm
Band4	NIR	780～920nm

Worldview-2,3 (WorldView-110 camera（WV110）)

バンド	Bandwidth	Wavelength
Band1	Visible Coastal	400～450nm
Band2	Visible Blue	450～510nm
Band3	Visible Green	510～580nm
Band4	\Visible Yellow	585～625nm
Band5	Visible Red	630～690nm
Band6	Red Edge	705～745nm
Band7	NIR_1	770～895nm
Band8	NIR_2	860～1040nm

Table 2. Specifications of satellite imagery data used

2.3 Atmospheric and geometric correction

The DN values of each band image data were converted to ground surface reflectance. In addition, the data used was subjected to atmospheric correction in order to calculate more accurate vegetation index values. ATCOR (Atmospheric Correction Software) created by DLR (Richter, R. (2010), Richter, R. et al. (2006)) was used for the atmospheric correction and conversion to ground surface reflectance. The converted image data was ortho-corrected using Rational Function Modeling (Yong, H., et al. (2004)) to ensure strict consistency with the geographic coordinate system. 5m DEM data from the National Land Digital Information published by the Geospatial Information Authority of Japan was used for the correction process here. This allowed the coordinates of the observation data for each observation year to be precisely superimposed. In addition, geospatial information of the afforestation area, which indicates the range of the analysis target, was superimposed.

2.4 Identifying reforestation areas

Polygon data showing reforestation areas was created based on the digital land information provided by the Geospatial Information Authority of Japan and the area maps of national and private forests published in the Forestry Agency and Miyagi Prefecture's reforestation restoration project materials. This polygon data was overlaid with satellite image data. From the results, vegetation index values calculated using satellite image data were extracted and tallied within the area, and the distribution characteristics of the vegetation index values in the reforestation areas were analyzed.

2.5 Calculation of NDVI and LAI

NDVI (Normalized Difference Vegetation Index) is a representative vegetation index value, and is calculated by the following formula (1).

$$NDVI = \frac{\rho_{IR} - \rho_R}{\rho_{IR} + \rho_R} \quad (1)$$

where ρ indicates the earth surface reflectance of each band. NIR indicates the near infrared region, and R indicates the visible red region. From the analysis of the relationship between the NDVI value obtained from the observation image of the high-resolution satellite Worldview-2 and the measured LAI value, the LAI estimation formula (2) was proposed in the previous research by Kokubo, Y. et al. (2020). In this study, the previously proposed formula (2) was cited.

$$LAI = 0.1e^{NDVI/0.179} \quad (2)$$

By substituting the NDVI value calculated by formula (1) into formula (2), the distribution of the estimated value of LAI in the afforestation area and the trend of the change in the time series were investigated. The spatial distribution of the calculated NDVI and LAI values within the afforestation area was mapped, and the time series changes in the distribution of the composition ratio of each index value within the afforestation area were also shown.

2.6 Display and consideration of changes in afforestation areas

The time-series change trends from before to after the disaster in the entire afforestation area and characteristic areas were investigated in detail by interpreting high-resolution satellite images. In addition, the damage to the coastal forest and the characteristics of the restoration process were evaluated from mapping showing the time-series changes in the spatial distribution of NDVI and LAI values in the entire afforestation area. In addition, a comparison of the characteristics of each index value was considered.

3. Results and Discussion

3.1 Survey by Satellite Image Interpretation

As shown in the image of the time series changes in the target area in Figure 3, sufficient luxuriant coastal forests were confirmed in 2010 before the tsunami disaster. The coastal forests suffered severe damage in the tsunami disaster in 2011, with trees falling and being washed away. A tendency was observed in which a lot of felling and land leveling work was carried out for new afforestation up to 2016, five years after the earthquake. After that, the planted trees were confirmed to gradually grow. In addition, a tendency was confirmed that the bare ground around the trees decreased as the trees grew. To confirm the time series changes in more detail, the change trends were grasped from the enlarged image shown in Figure 4. As shown in the figure, severe damage was confirmed immediately after the disaster in both the coastal forest along the coastline (area A, private forest area) and the coastal forest slightly inland from the coastline (area B, national forest area). However, it was confirmed that the disappearance and washout of coastal forests in Area B was more noticeable. This difference was thought to be due to differences in the species of coastal forests, their maintenance status, and the progression of the tsunami. After the disaster, land leveling work was carried out first in Area B in order to restore new coastal forests. After that, the coastal forests that had remained in Area A since the time of the disaster were artificially cut down, and land leveling work for new reforestation was carried out. by 2016, land leveling work in all reforestation areas was almost complete, and new reforestation had begun. After that, the process of reforestation being restored over time was confirmed from the images.

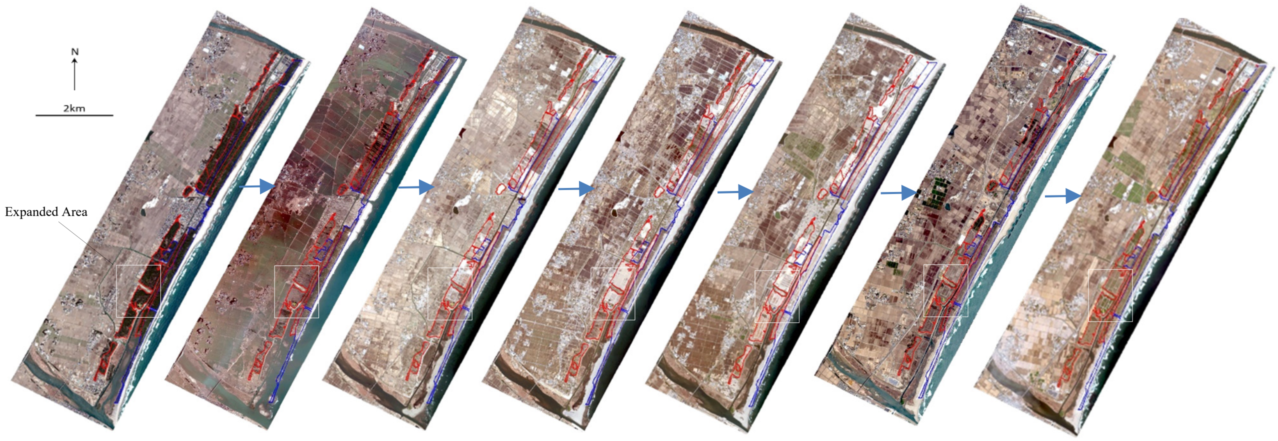

(a)2010/04/04 1 year before the disaster
(b)2011/03/14 3 days after the disaster
(c)2013/04/14 2 years after the disaster
(d)2014/04/02 3 years after the disaster
(e)2016/04/13 5 years after the disaster
(f)2020/04/08 9 years after the disaster
(g)2023/03/31 12 years after the disaster

Figure 3. Changes in landcover condition in the entire area before and after the disaster (True color composite display)

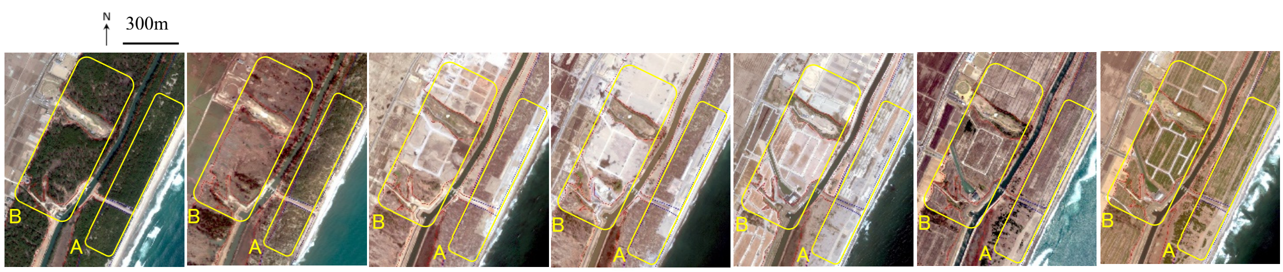

(a)2010/04/04 1 year before the disaster
(b)2011/03/14 3 days after the disaster
(c)2013/04/14 2 years after the disaster
(d)2014/04/02 3 years after the disaster
(e)2016/04/13 5 years after the disaster
(f)2020/04/08 9 years after the disaster
(g)2023/03/31 12 years after the disaster

Figure 4. Interpretation of land cover changes over an expanded area (True color composite display)

3.2 Time series changes in NDVI

Figure 5 shows the time series changes in the NDVI distribution over the entire afforestation area. Figure 7 shows the time series change of NDVI distribution shown by the composition ratio in the afforestation area. As shown in the figure, very high NDVI values were distributed throughout the afforestation area before the disaster, and it was confirmed that highly active coastal forests were widely maintained. In 2011, immediately after the disaster, many coastal forests were fallen or lost in the afforestation area, and a sudden drop in NDVI values was confirmed in many places in the afforestation area. Until 2016, the NDVI value continued to decrease due to the progress of land preparation work for new afforestation, and since then, a gradual increase in NDVI values was confirmed due to the start of new afforestation. This was also confirmed by the change in the composition ratio shown in Figure 7. To confirm the changes in more detail, the trends in the distribution of NDVI values were identified from the enlarged image shown in Figure 6. Immediately after the disaster, the distribution of high NDVI values was confirmed in the coastal forests along the coastline (area A, private forest area) that survived the disaster. In contrast, in the coastal forests slightly inland from the coastline (area B, national forest area), an extreme drop in NDVI values was confirmed due to the severe loss of coastal forests due to the tsunami. After that, land preparation work for new afforestation was carried out first in area B, so the NDVI values remained low until 2016, when land preparation was almost completed. During this period, a downward trend in the NDVI values of the remaining coastal forests in area A was also confirmed. In 2016, land preparation work was almost completed in areas A and B, resulting in a distribution of low NDVI values indicating bare ground over a wide area. Subsequently, since 2020, new afforestation has begun, and it has been confirmed that gradually higher NDVI values are being distributed in neat plantation shapes within the afforestation areas.

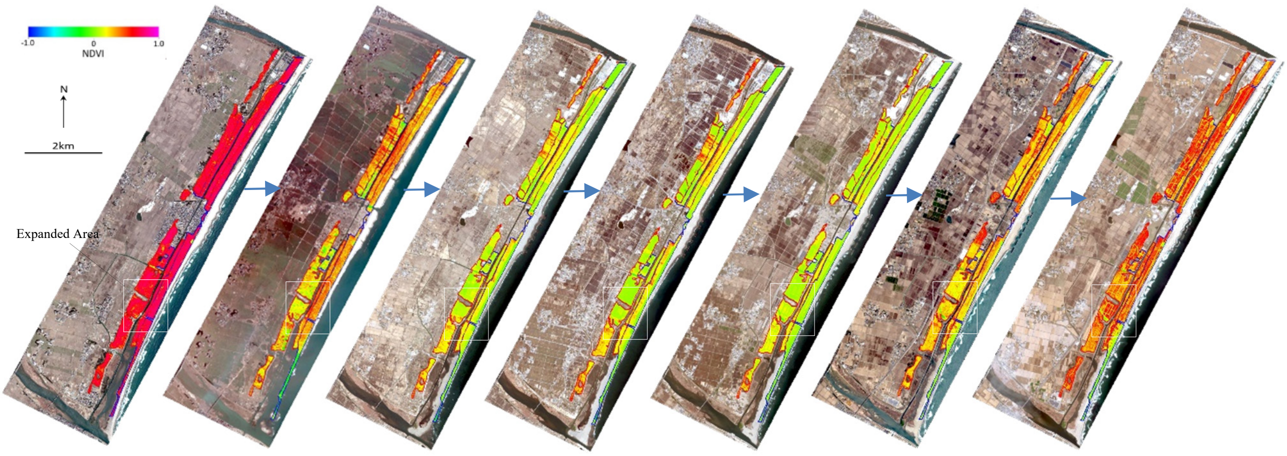

(a)2010/04/04 1 year before the disaster | (b)2011/03/14 3 days after the disaster | (c)2013/04/14 2 years after the disaster | (d)2014/04/02 3 years after the disaster | (e)2016/04/13 5 years after the disaster | (f)2020/04/08 9 years after the disaster | (g)2023/03/31 12 years after the disaster

Figure 5. Changes in NDVI distribution across the afforestation area before and after the disaster

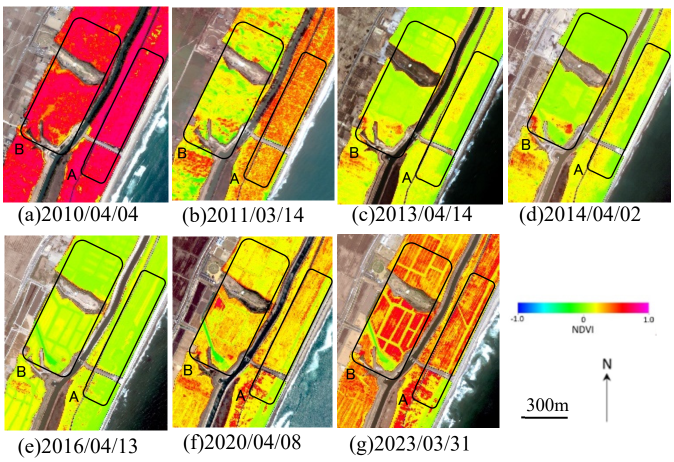

Figure 6. Changes in NDVI distribution over an expanded area

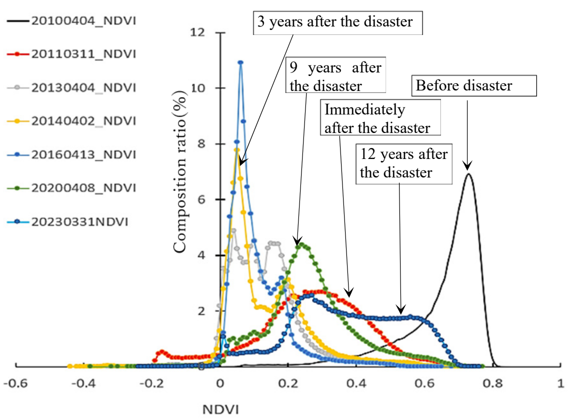

Figure 7. Time series changes in the composition ratio of NDVI in the entire afforestation area

Proceedings of the International Cartographic Association, 7, 24, 2025 | https://doi.org/10.5194/ica-proc-7-24-2025
32nd International Cartographic Conference (ICC 2025), 17–22 August 2025, Vancouver, Canada.

3.3 Time series changes in LAI

Figure 8 shows the time series change of LAI distribution in the entire afforestation area. Figure 10 shows the time series change of LAI distribution shown by the composition ratio in the entire afforestation area. As shown in the figure, before the disaster, there were many high LAI value distributions, confirming the health of the coastal forest. Immediately after the disaster, an extreme decrease in LAI value due to fallen and lost trees was confirmed. After that, the tendency of LAI to decrease continued for several years due to land preparation work for new afforestation. In 2023, the growth of the newly planted forest around 2016 progressed slowly, and the tendency of LAI value gradually increasing was confirmed. This was also confirmed from the change trend of the composition ratio shown in Figure 10. In order to confirm the time series change in more detail, the change trend of LAI value distribution was grasped from the enlarged image shown in Figure 9. Immediately after the disaster, in coastal forests along the coastline (area A, private forest area), many coastal forests remained standing despite the disaster and the foliage still remained, so a private relatively high LAI value distribution was confirmed in many places. In contrast, in coastal forests slightly inland from the coastline (area B, national forest area), an extreme drop in the LAI value distribution was confirmed in many places due to the severe loss of coastal forests due to the tsunami. After that, in both areas A and B, the distribution of low LAI values indicated bare ground during the period when land leveling work for new afforestation continued. After that, around 2020, new afforestation began, and the NDVI value showed a tendency to increase in part in advance, and then in 2023, a gradual increase in LAI values was confirmed due to the gradual increase in leaf area as the trees grew. In this way, differences arose between the time when NDVI values and the time when LAI values increased depending on the time when afforestation began and the subsequent progress of leaf growth, and it was considered that investigations of the forest restoration process could be evaluated in more detail.

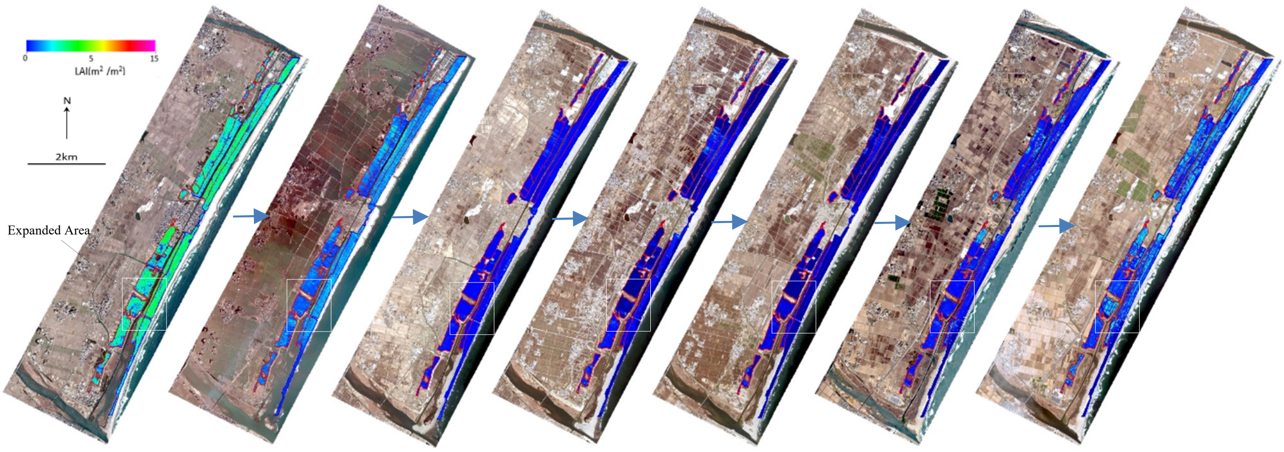

(a)2010/04/04 1 year before the disaster | (b)2011/03/14 3 days after the disaster | (c)2013/04/14 2 years after the disaster | (d)2014/04/02 3 years after the disaster | (e)2016/04/13 5 years after the disaster | (f)2020/04/08 9 years after the disaster | (g)2023/03/31 12 years after the disaster

Figure 8. Changes in LAI distribution across the afforestation area from before to after the disaster

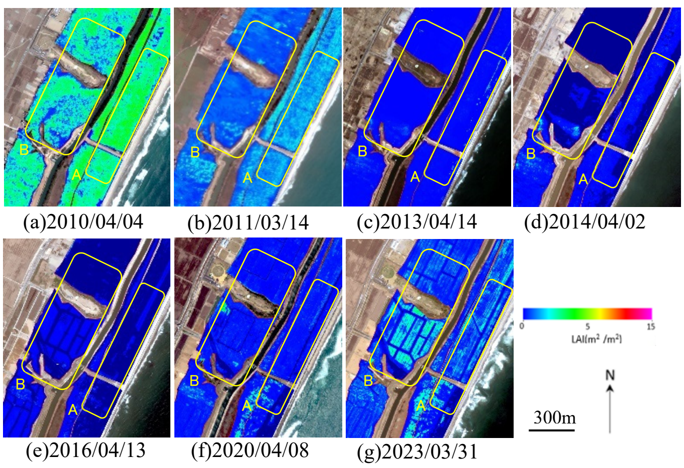

Figure 9. Changes in NDVI distribution over an expanded area

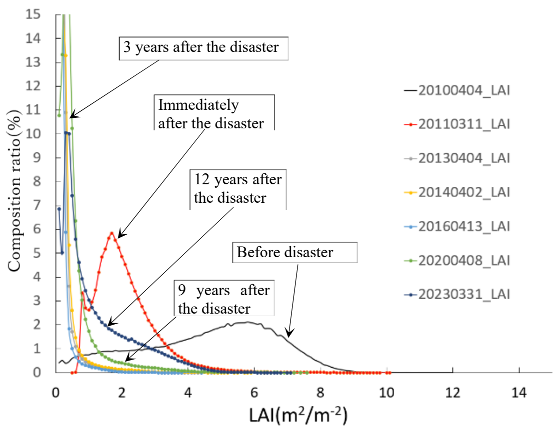

Figure 10. Time series changes in the composition ratio of LAI in the entire afforestation area

Proceedings of the International Cartographic Association, 7, 24, 2025 | https://doi.org/10.5194/ica-proc-7-24-2025
32nd International Cartographic Conference (ICC 2025), 17–22 August 2025, Vancouver, Canada.

4. Conclusions

The damage and restoration process of coastal forests in the Sendai Plain before and after the Great East Japan Earthquake and for about 12 years thereafter was investigated in detail by analyzing time-series high-resolution satellite image data. The normalized difference vegetation index (NDVI) using the spectral characteristics of high-resolution satellite image data and the leaf area index (LAI) estimated from the NDVI value were used to effectively analyze the characteristics of the restoration process of coastal forests by new afforestation after damage. The NDVI value showed that the vegetation activity before the disaster suddenly decreased due to the disaster, and then gradually increased due to the long-term restoration process of afforestation. Similarly, the LAI value showed that the process of restoration from the loss of leaf area of coastal forests was gradually achieved through long-term restoration work by spatial mapping. In addition, the possibility of understanding the growth process of forests in more detail was considered based on the characteristics of the time-series difference in the increasing trend of NDVI and LAI values associated with the growth of new afforestation. By using a combination of these forest-related index values in the survey, trends of change could be considered more effectively. In the future, studies will be conducted to further improve the accuracy and interpretation of the various index values, and by continuing time-series monitoring of the target area, it is thought that more appropriate support information for future afforestation plans will be developed from high-resolution spatial mapping using a variety of index values. It is also thought that this method can be effectively used to support future disaster prevention, mitigation, and natural environment improvement in other coastal areas with coastal forests.

5. Acknowledgements

The Worldview-2,3 and GeoEye-1 images used in this study include copyrighted material of MAXAR, Inc., All Rights Reserved.

6. References

Cabinet Office Emergency Disaster Response Headquarters. Regarding the 2011 off the Pacific coast of Tohoku Earthquake (Great East Japan Earthquake). https://www.bousai.go.jp/2011daishinsai/pdf/torimatome20240308.pdf（accessed 2024/03/31)

Forestry Agency, Tohoku Regional Forest Office. Restoration of coastal disaster prevention forests - Damage and restoration caused by the 2011 off the Pacific coast of Tohoku Earthquake and the massive tsunami. https://www.rinya.maff.go.jp/tohoku/koho/saigaijoho/pdf/bousairin_pamphlet.pdf (accessed 2023/12/10).

Forestry Agency Tohoku Regional Forest Office. Restoration and Regeneration of Coastal Disaster Prevention Forests. https://www.rinya.maff.go.jp/tohoku/koho/ saigaijoho/pdf/h24_11_sendaiwan.pdf (accessed 2024 / 01/10).

Geospatial Information Authority of Japan. Base map information (digital elevation model). https://fgd.gsi.go.jp/download/ref_dem.html (accessed 2024/01/10).

Geospatial Information Authority of Japan. Responses of the Geospatial Information Authority of Japan, Immediately After the Great East Japan Earthquake. https://www.gsi.go.jp/BOUSAI/h23_tohoku_chokugo.html (accessed 2023/12/01).

Hashiba, H., Sugimura, T., Aoyama, S. and Asaka, T. (2015). Analysis of change after damage to coastal woods on the Sendai plains of Miyagi prefecture using high-resolution satellite remote sensing. In: *Journal of Japan Society of Civil Engineers, Ser. B3 (Ocean Engineering)*, Vol.71, 2, I_999-I_1004, 2015, https://doi.org/10.2208/jscejoe.71.I_999.

Hashiba, H. and Sonobe, M. (2024). Time-series monitoring of the regeneration process of tsunami affected coastal forests through comparative study of multiple vegetation indexes using near-infrared high-resolution satellite images. In: *Proceedings of SPIE, Optical Engineering + Applications 2024, Infrared Remote Sensing and Instrumentation XXXII*, Vol.131440U, https://doi.org/10.1117/12.3027608.

Hoshi, N., Tatsuhara, S. and Abe, N. (2001). Estimation of leaf area index in natural deciduous broad-leaved forests using Landsat TM data. In: *Jornal of the Japanese Forestry Society*, Vol. 83, 4, 315-321, 2001, https://doi.org/10.11519/jjfs1953.83.4_315.

Jiang, Z., Huete, A.R., Didan, K. and Miura, T. (2008). Development of a two-band enhanced vegetation index without a blue band. In: *Remote Sensing of Environment*, Vol.112, 3833 - 3845. 2008, https://doi.org/10.1016/j.rse.2008.06.006.

Kimm, H. and Ryu, Y. (2015). Seasonal variations in photosynthetic parameters and leaf area index in an urban park. In: *Urban Forestry & Urban Greening*, Vol.14, 4, 1059-1067, 2015, https://doi.org/10.1016/j.ufug.2015.10.003.

Kokubu, Y., Hara, S. and Tani, A. (2020). Mapping Seasonal Tree Canopy Cover and Leaf Area Using Worldview-2/3 Satellite Imagery: A Megacity Scale Case Study in Tokyo Urban Area. In: *Remote Sensing*, MDPI, Vol.12, 9, 1505, 2020, https://doi.org/10.3390/rs-12091505.

Ministry of Land, Infrastructure, Transport and Tourism. Records of the Great East Japan Earthquake - Ministry of Land, Infrastructure, Transport and Tourism's Disaster Response. https://www.mlit.go.jp/saigai/kirokusyu.html (accessed 2024/01/10)

Miyagi Prefecture Fisheries and Forestry Department, Forest Management Division. Guide to Coastal Disaster Prevention Forest Management. https://www.pref.miyagi.jp/documents/37766/tebikiver2.pdf (accessed 2024/01/10).

Qi, J., Chehbouni, A., Huete, A. R., Kerr, Y. H. and Sorooshian, S. (1994). A Modified Soil Adjusted Vegetation Index. In: *Remote Sensing of Environment*, Vol. 48, 2, 119-126, 1994, https://doi.org/10.1016/0034-4257(94)90134-1.

Richter, R. (2010). Atmospheric / Topographic Correction for Satellite Imagery - ATCOR2/3 User Guide. DLR - German Aerospace Center, 1-165, 2010.

Richter, R., Schläpfer, D. and Müller, A. (2006). An automatic atmospheric correction algorithm for visible / NIR imagery. In: *International Journal of Remote Sensing*, Vol.27, 10, 2077-2085, 2006, https://doi.org/10.1080/01431160500486690.

Rouse, J.W., Haas, R. H., Schell, J. A., Deering, D. W., and Harlan, J. C. (1974). Monitoring the vernal advancement and retrogradation (green wave effect) of natural vegetation. In: Remote Sensing Center, Texas A&M University/GODDARD SPACE FLIGHT CENTER, Document ID:19750020419.

Sonobe, M. and Hashiba. H. (2018). Evaluation of restoration process around the coastal area of Sendai coast using time-series high-resolution satellite image. In: *Journal of Japan Society of Civil Engineers, Ser. B3 (Ocean Engineering)*, Vol.74,2, I_139-I_144, 2018, https://doi.org/10.2208/jscejoe.74.I_139.

Yong, H., Tao, V. and Croitoru, A. (2004). Understanding the rational function model: Methods and applications. In: *International Archives of Photogrammetry and Remote Sensing*, XXXV (4), 423, 2004, https://www.isprs.org/proceedings/XXXV/congress/comm4/papers/423.pdf.